Metrol. Meas. Syst., Vol. XXI (2011), No. 3, pp. 447–460.

PAN POLSKA AKADEMIA NAUK

METROLOGY AND MEASUREMENT SYSTEMS

Index 330930, ISSN 0860-8229

www.metrology.pg.gda.pl

M&MS

SYSTEMATIC ERROR OF ACOUSTIC PARTICLE IMAGE VELOCIMETRY AND ITS CORRECTION

Witold Mickiewicz

West Pomeranian University of Technology, Szczecin, Faculty of Electrical Engineering, ul. Sikorskiego 31, 70-313 Szczecin, Poland (✉ witold.mickiewicz@zut.edu.pl, +48 91 449 5205)

Abstract

Particle Image Velocimetry is getting more and more often the method of choice not only for visualization of turbulent mass flows in fluid mechanics, but also in linear and non-linear acoustics for non-intrusive visualization of acoustic particle velocity. Particle Image Velocimetry with low sampling rate (about 15Hz) can be applied to visualize the acoustic field using the acquisition synchronized to the excitation signal. Such phase-locked PIV technique is described and used in experiments presented in the paper. The main goal of research was to propose a model of PIV systematic error due to non-zero time interval between acquisitions of two images of the examined sound field seeded with tracer particles, what affects the measurement of complex acoustic signals. Usefulness of the presented model is confirmed experimentally. The correction procedure, based on the proposed model, applied to measurement data increases the accuracy of acoustic particle velocity field visualization and creates new possibilities in observation of sound fields excited with multi-tonal or band-limited noise signals.

Keywords: particle image velocimetry, acoustic measurement, acoustic particle velocity, sound field analysis.

1. Introduction

Particle Image Velocimetry (PIV) is a non-intrusive technique for simultaneously measuring the velocities at many points in a fluid flow. The velocity is evaluated in an indirect way using measured particle displacement. In the case of an acoustic field the measured quantity is the acoustic particle instantaneous displacement and velocity.

To register medium displacements the fluid is seeded with tracer particles and the region under investigation is illuminated. An image of the illuminated region is captured and then, a short time interval later, a second image is taken. Suitable correlation analysis of these images yields an instantaneous displacement vector map. The time interval between acquisitions of the consecutive particle images is known (it can be chosen as a measurement parameter), thus the calculated displacement map can be transformed into the velocity vector map using the formula:

$$\vec{v} = \frac{\vec{s}}{\Delta t} \quad . \tag{1}$$

The accuracy of velocity field evaluation in this way depends: on physical phenomena occurring in the field (accelerations, vortices etc.), on accuracy in evaluation of the displacement field $\vec{s}$ and on the time interval Δt (duration time).

Many authors address in their papers the PIV accuracy analysis as a function of optical system parameters, seeding particle size and density or the correlation algorithm used. Two

Article history: received on Nov. 07, 2013; accepted on Mar. 10, 2014; available online on Sep. 15, 2014; DOI: 10.2478/mms-2014-0038.

main approaches dominate: analytic model-based [1–2] and computer simulations using Monte Carlo analysis [3–4]. The mentioned papers address the PIV technique applied to visualize mass flows in fluid mechanics and some conclusions are universal (e.g. optimal seeding particle size and density) but other cannot be directly used in case of the acoustic field where particles vibrate and move over closed trajectories. On the other side, specific features of acoustic particle movements can be used as *a priori* knowledge to create a specific model of the measurement procedure. On that base the systematic error can be assessed.

In the paper the developed model of systematic error due to non-zero value of time interval Δt is presented. Experimental results validate the proposed amplitude and phase corrections. The presented method allows more accurate phase-locked PIV mapping of acoustic waves generated by pure tones and also multitonal or band-limited excitation.

2. PIV visualization error of acoustic velocity due to non-zero Δt value

2.1. The problem of optimum time interval Δt selection

In a measuring procedure with PIV technique the user has to choose the time interval Δt. The choice - especially when PIV is applied to an acoustic field - influences the measurement results. Fig. 1 shows three pairs of instantaneous acoustic velocity fields measured in a waveguide for pure tone excitation of 255 Hz, 3227 Hz and 6454 Hz. In each pair the same time constant was observed in reference to the excitation signal period, but the PIV measurement was made using a different time interval Δt. Three main differences can be seen in the presented figures: for shorter Δt the estimated velocity values (vector lengths) are higher, upper distributions are shifted in space referring to the lower, lower images seem to be more smooth then the upper ones. So it is obvious that time interval Δt value influences the time-space reconstruction of the acoustic field and should be chosen using precisely established criteria.

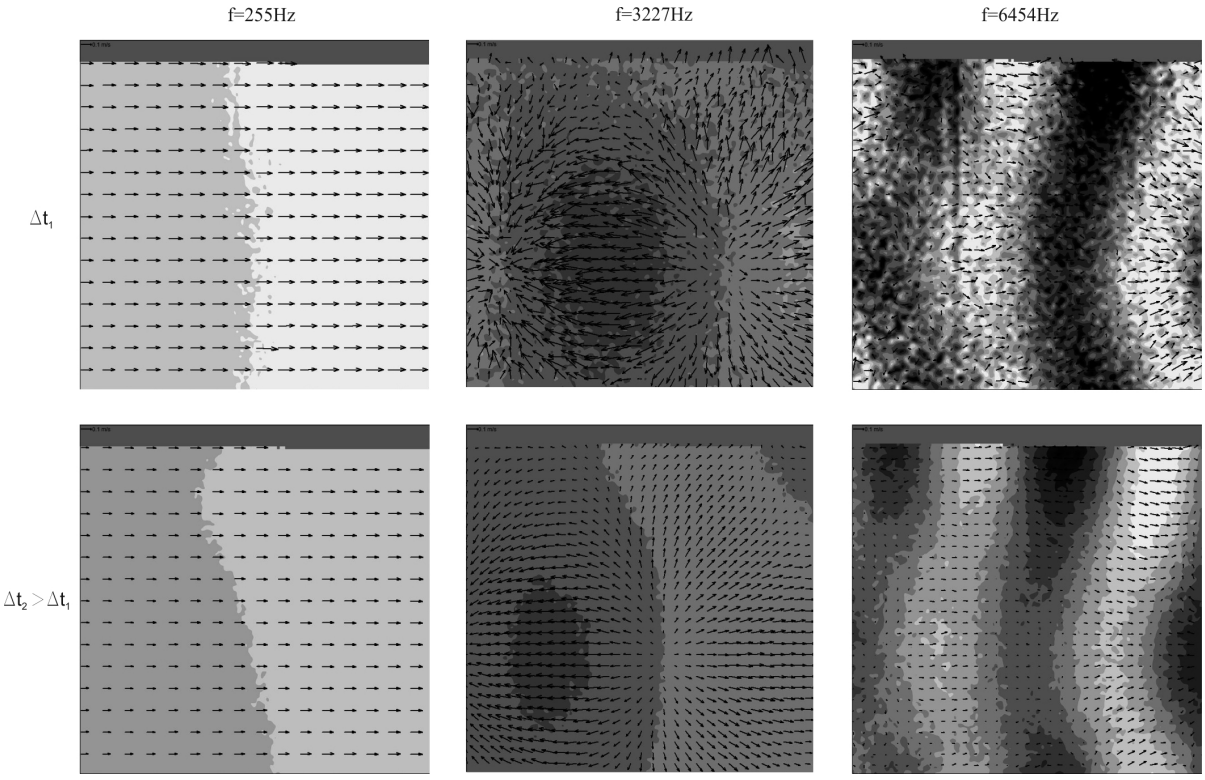

Fig. 1. The samples of acoustic velocity fields in a waveguide for various excitation frequencies measured with a PIV system with two values of time interval Δt.

The Δt optimization for acoustic PIV measurements with pure tone excitation was addressed in several publications. Here some thoughts from [5] are presented, where the authors pointed out two phenomena determining optimal Δt choice in the case of experiments with acoustic excitation. On the one hand the time interval Δt has to be long enough, that the change in spatial position of the moving particle could be detected and evaluated quantitatively by the PIV system used. This spatial resolution of the system is connected with the camera resolution, the size of seeding particles and the algorithms used for subpixel displacement evaluation. On the other hand the time interval Δt should be short enough to fulfil the assumption of velocity constancy over this time. During Δt the seeding particles could not also go outside the interrogation area analyzed by the correlation algorithm. The cited authors have presented the visualization of the velocity field in front of the outlet of a bass-reflex loudspeaker enclosure. The experiments were done with pure tone excitation with frequencies of 25Hz, 72Hz and 144Hz. Basing on the comparison between the experimental results and theoretical calculations, where an electro-dynamic model of the loudspeaker was applied, they proposed the formula:

$$\frac{1}{2}\frac{\delta_{pix}}{U_{ac}} < \Delta t < 0.12 T_{ac}\,, \tag{2}$$

where: δ_{pix} - pixel size, U_{ac} - acoustic velocity amplitude calculated from the driving voltage using a theoretical loudspeaker model and T_{ac} - excitation tone period.

For the chosen frequencies the particle displacements are big in relation to the reported interrogation areas even for sound pressure levels below 120 dB. The mentioned increase of error values for longer Δt intervals can be really caused by the particle displacements which were too large in reference to the interrogation area size. For higher frequencies and lower levels the displacements decrease and the upper limit of the time interval could be increased. The problem of velocity constancy over Δt can be reduced using *a priori* knowledge about the sinusoidal form of the propagating wave. This approach is shown in the paper.

2.2 Systematic error model of PIV acoustic velocity measurement due to non-zero Δt value

During acoustic wave propagation, the seeding particles vibrate consistently with air molecules and their movements - registered by the PIV system in the plane formatted by light knife optics - can be identified with movements of acoustic particles. The term "acoustic particle" is widely used in theoretical acoustics and describes a small, comparing with the wavelength, volume of fluid (air), which consists of many medium-size molecules. In the plane of observation a trajectory of acoustic particle displacement has got the shape of an ellipse (or even straight line) and we can decompose the displacement vector $\vec{s}$ into two orthogonal components:

$$\vec{s} = s_x \cdot \vec{\mathrm{e}}_\mathrm{X} + s_Y \cdot \vec{\mathrm{e}}_\mathrm{Y}\,, \tag{3}$$

$$s_x = s_{X\max} \cdot \sin(\omega \mathrm{t} + \varphi_{\mathrm{X0}})\,, \tag{4}$$

$$s_Y = s_{Y\max} \cdot \sin(\omega \mathrm{t} + \varphi_{\mathrm{Y0}})\,, \tag{5}$$

where: $\vec{\mathrm{e}}_\mathrm{X}, \vec{\mathrm{e}}_\mathrm{Y}$ - unit vectors in Cartesian coordinate system; s_X, s_Y - orthogonal components

of instantaneous displacement; $s_{X\max}$, $s_{Y\max}$ - orthogonal component amplitudes; ω - angular frequency of the harmonic signal; φ_{X0} , φ_{X0} - initial phases of instantaneous displacement.

To simplify the description in the following text only the X-component will be considered - the Y-component is transformed in the same way - and the X index will be omitted. According to (1) in Eulerian approach the component of the instantaneous velocity in the observation point during the harmonic movement can be described as:

$$v_{IDEAL} = \frac{ds}{dt} = \omega \cdot s_{X\max} \cdot \cos(\omega t + \varphi_{X0}) . \tag{6}$$

According to the principles of operation of the PIV technique, the velocity (6) for time instant t_0 will be measured as:

$$v_{MEAS} = \frac{s_{X\max} \cdot (\sin(\omega(t_0 + \Delta t) + \varphi_{X0}) - \sin(\omega t_0 + \varphi_{X0}))}{\Delta t} . \tag{7}$$

When we use the definition of Sa(x) function:

$$\mathrm{Sa}(x) \equiv \frac{\sin(x)}{x} \tag{8}$$

(7) can be rewritten in the following form:

$$v_{MEAS} = \omega \cdot s_{X\max} \cdot \mathrm{Sa}(\frac{\omega \Delta t}{2}) \cdot \cos(\omega t_0 + \frac{\omega \Delta t}{2} + \varphi_0) . \tag{9}$$

Comparing (6) and (9) we can see that the harmonic signal reconstructed on the basis of a PIV measurement yields distorted amplitude and phase. The multiplicative amplitude error factor ε_{amp} will be:

$$\varepsilon_{amp} = \frac{v_{MEAS}}{v_{IDEAL}} = \mathrm{Sa}(\frac{\omega \Delta t}{2}) = \mathrm{Sa}(\pi \frac{\Delta t}{T}) , \tag{10}$$

and the additive phase error factor ε_{phase} will be:

$$\varepsilon_{phase} = \varphi_{MEAS} - \varphi_{IDEAL} = \frac{\omega \Delta t}{2} = \pi \frac{\Delta t}{T} , \tag{11}$$

where T is a period of the measured harmonic signal.

The effect of amplitude decrease and phase shift of the reconstructed sinusoidal signal for different $\frac{\Delta t}{T} > 0$ values compared with the ideal case is shown in Fig. 2.

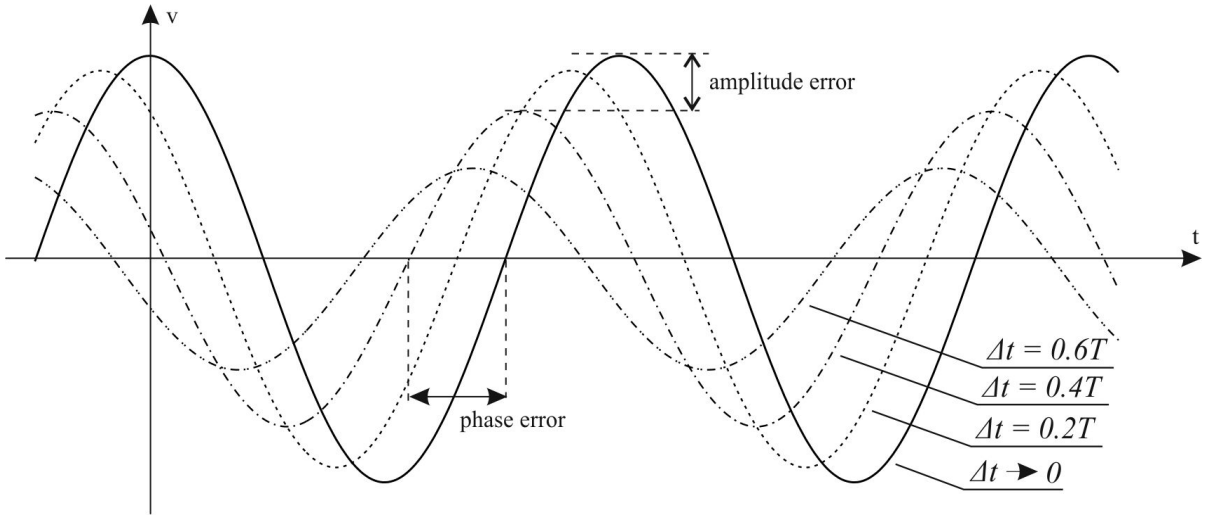

Fig. 2. The effect of amplitude drop and phase shift of measured acoustic velocity v for various time intervals $\Delta t > 0$ expressed as a fraction of signal period T in reference to an ideal case.

In Table 1 some numerical values of ε_{amp} and ε_{phase} are collected. These values may be applied to correct the measurement results. It will be shown in the next paragraph.

Table 1. The numerical values of ε_{amp} and ε_{phase}.

$\frac{\Delta t}{T}$	ε_{amp}	20 log ε_{amp} [dB]	ε_{phase} [rad]	$\frac{\Delta t}{T}$	ε_{amp}	20 log ε_{amp} [dB]	ε_{phase} [rad]
0	1.000	0.0	0.0000	0.26	0.893	-1.0	0.4084
0.02	0.999	0.0	0.0314	0.28	0.876	-1.1	0.4398
0.04	0.997	0.0	0.0628	0.3	0.859	-1.3	0.4712
0.06	0.994	-0.1	0.0942	0.32	0.840	-1.5	0.5027
0.08	0.990	-0.1	0.1257	0.34	0.821	-1.7	0.5341
0.1	0.984	-0.1	0.1571	0.36	0.800	-1.9	0.5655
0.12	0.977	-0.2	0.1885	0.38	0.779	-2.2	0.5969
0.14	0.968	-0.3	0.2199	0.4	0.757	-2.4	0.6283
0.16	0.958	-0.4	0.2513	0.42	0.734	-2.7	0.6597
0.18	0.948	-0.5	0.2827	0.44	0.711	-3.0	0.6912
0.2	0.936	-0.6	0.3142	0.46	0.687	-3.3	0.7226
0.22	0.922	-0.7	0.3456	0.48	0.662	-3.6	0.7540
0.24	0.908	-0.8	0.3770	0.5	0.637	-3.9	0.7854

2.3 Procedure of amplitude and phase correction of measurement data for multitonal and band-limited acoustic excitation

As it was shown in the previous section, the systematic error introduced to the velocity measurement using a PIV system due to non-zero Δt value depends on the $\Delta t/T$ ratio, where T is the period of the pure tone excitation. We can keep the error on the same level, if for the tones with various frequencies we adjust the interval Δt value to retain a constant $\Delta t/T$ ratio. This conclusion remains in agreement with [12]. It is worth to mention that in the literature known to the author the presented research concerned only the pure tone excitations with various frequencies and levels. In case of multitonal or band-limited noise excitation, or observation of non-linear distortions, where the signal shape is no more sinusoidal, each harmonic component will be measured with a different $\Delta t/T$ ratio. In such cases the measured wave will be distorted due to shifts in amplitude and phase of each reconstructed harmonic component. Using the presented model we can apply correction coefficients to obtain more reliable wave shape reconstruction. The measurement of the acoustic velocity field with correction procedure should encompass the following steps:

1. Phase-locked PIV measurement using $\Delta t = 1/2T$, where T is the period of the highest frequency component in the excitation signal spectrum. The number of recorded phase steps should ensure sufficient resolution for the FFT analysis of the reconstructed signal.
2. Estimation of amplitudes and phases of frequency components in the measured signal using FFT analysis.
3. Correction of amplitudes and phases using different model coefficient values depending on the frequency.
4. Synthesis of the signal time form using corrected harmonic components.

The procedure was evaluated experimentally. In the case of real measurements the $\Delta t/T$ value should satisfy the sampling theorem to properly sample the particle displacements, which in general could follow a more complex trajectory than a simple ellipse. Therefore $\Delta t/T$ should be limited and be less than 0.5, where T is the period of the maximum frequency component in the signal.

The correlation between the theoretical model and measurement data and the application of the proposed correction procedure to real measurement data, which can be used to improve the accuracy of acoustic waveform reconstruction in the case of dual-tone excitation, will be demonstrated in the next sections. Some technical aspects of measurement methodology and used setup will be introduced before the experimental results presentation.

3. Measurement methodology and setup

3.1 Phase-locked Particle Image Velocimetry

Until recently, restrictions in the rate at which images could be captured have limited the PIV technique to the analysis of slow flows. However, advances in camera technology and development of synchronized image acquisition procedures have now opened up the possibility of using PIV in the analysis of faster flows. Indeed, image capture rates are now fast enough to enable two images to be captured during a fraction of an acoustic cycle, indicating the potential for using PIV to analyse sound fields. Nowadays time-resolved PIV systems ensure recording rates up to tens of kilohertz with 1000 pixel x1000 pixel spatial resolution. When higher spatial resolution is needed, phase-locked PIV can be used in cases

where image acquisition can be synchronized with the excitation signal. The latter method will be described and used in the paper.

The measurement of instantaneous acoustic particle velocity in successive phases of acoustic signal evolution, which satisfy the Shannon sampling theorem, is realized by multiple data acquisition in the instants of time being in controlled time relation (synchronization) to the periodical excitation signal. Fig. 3 shows this idea. Time T_{SS} is the period of the signal which triggers the acquisition process of the first image. It is synchronized with the excitation signal which forces the investigated acoustic energy flow. The minimum value of T_{SS} is restricted by the performance of the PIV system, especially by maximum repetition rate of the laser and image acquisition. A camera takes the first image after time T_D since trigger, when the Laser 1 generates its light pulse. After interval Δt , Laser 2 generates its light pulse and the camera takes a second image. Now some time is needed for transferring image data to computer and for laser charging. After T_{SS} ,the acquisition process repeats (Fig. 3A). To ensure high signal-to-noise ratio in the measured velocity field, for one T_D value tens to a hundred picture pairs are recorded. The exact number of collected pairs is strictly connected with the excitation signal level. The next value of T_D is set after collection of a suitable number of images at the previous T_D value and the process repeats (Fig. 3B). The number of recorded phases for one excitation signal cycle depends on experiment goals and required accuracy. If we use a simple tone as an excitation signal, phase number is about a few to tens [6–9]. Many authors mention the use of phase-locked PIV in their investigation of hydrodynamic field excited acoustically [10–13].

3.2 Experimental set-up

For experimental part of the research the planar PIV system supplied by LaVision GmbH (Goettingen Germany) was used. On this framework an experimental stand was developed. The overview of the experimental set up is shown in Fig. 4.

The acoustic velocity field was observed in an acoustic duct – a Plexiglas channel of square cross-section. The inner dimensions of the cross-section were 150mm x 150 mm. The walls of the channel are 8 mm thick. The measurements were made in a plane parallel to the channel length at the mid-channel location.

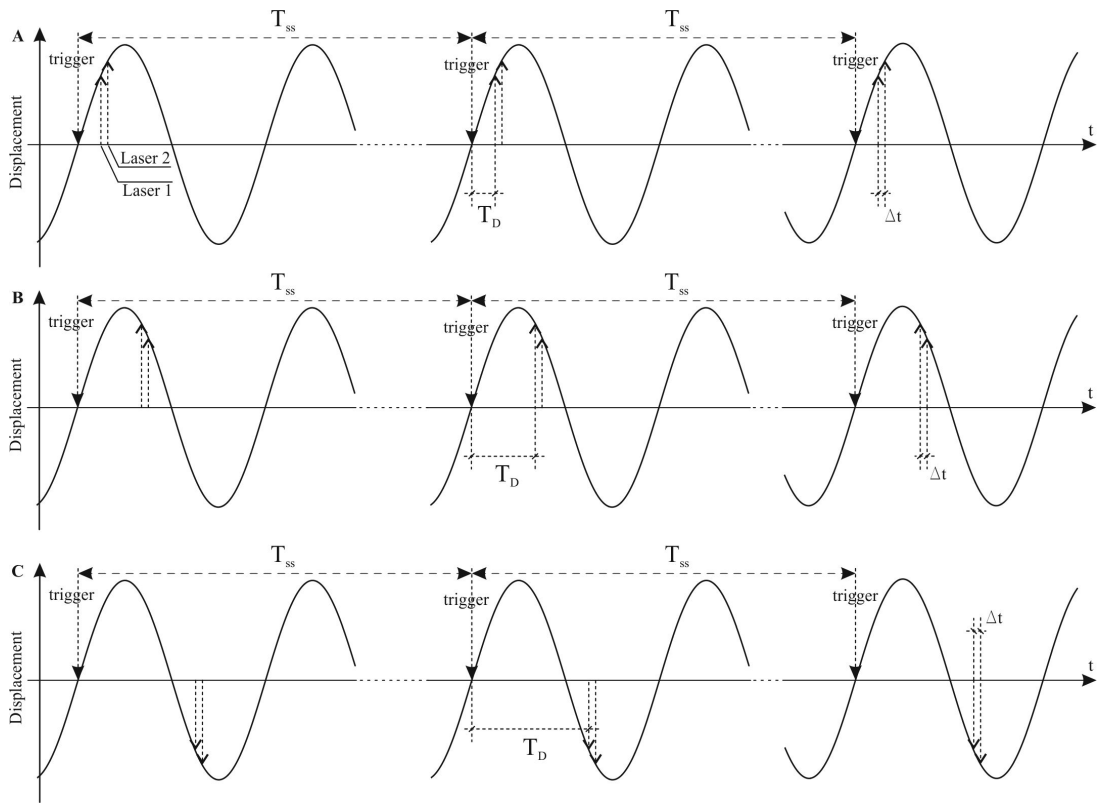

Fig. 3. Synchronized image acquisition in phase-locked PIV for different signal phases, where T_{ss} – period of the image pair acquisition process; T_D – adjustable delay between trigger signal and Laser 1 pulse (first image acquisition); Δt – time interval between image acquisition in one pair.

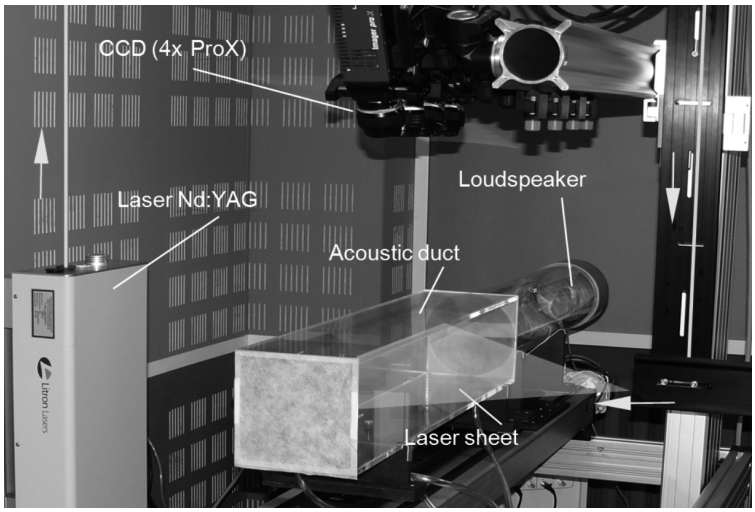

Fig. 4. Experimental setup with PIV measurement system.

The presented PIV system contains as a light source a Litron laser model Nano TRL 325-15. This is a Nd:YAG laser with a maximum pulse energy of 325mJ. A digital 4-megapixel CCD camera (LaVision Imager Pro X 4M) with a resolution of 2048 x 2048 pixels was used to acquire flow images. The field of view of the camera with the optics used was 120 mm x 120mm. The camera was connected to a PC equipped with a frame grabber (Matrox Solios eCL CameraLink) that received 14 bit images at a rate of 15 Hz (7 Hz rate for image pairs). LaVision Programmable Synchronisation Unit 9 was used to control the timing of the laser pulses and synchronize the acquisition to the excitation signal. Di-Ethyl-Hexyl-

Sebacat (DEHS oil, ρ_{DEHS} = 912 kg m^{-3}) and a LaVision aerosol generator was used to produce a mist of seeding particles with a mean diameter of 1μm. The acoustic wave in the duct was excited using a Tonsil GDN 13/40/8 loudspeaker localized at the end of a 1.5m long channel. The use of a loudspeaker supplied by a power amplifier (CROWN XLS2000, output power 2x375W) makes it easy to adjust the frequency and intensity of excitation. A function generator Agilent 33210A as well as computer-based ProTools Digital Audio Workstation was used to generate the sinusoidal and duotonal signals. The acoustic pressure was monitored by a SVANTEC SVAN 958 sound analyzer. For pure tone excitation the acoustic pressure level was measured in the first pressure anti-node between the examined area and open outlet of the waveguide.

The instantaneous acoustic velocity fields were calculated from the collected seeding particles image pairs using DaVis 8.11 software. The computational algorithm used an interrogation area of 32 x 32 pixels with 50% overlap. As the calculation result a vector field of 128 x 128 velocity vectors (about 1 vector per 1 mm^2 of the field of view) was obtained for each acquisition phase. Each vector was described by two orthogonal velocity components.

Before experiments the calibration procedure of optical system was performed using a calibration plate supplied with the system. The procedure was applied according to steps provided by DaVis software. The accuracy of seeding particle displacement is of about 0.17 pixel with the pixel size of 7.4 μm. It gives a displacement accuracy of 1.3 μm. The accuracy of velocity evaluation depends on time interval Δt.

The maximum frequency used in the presented research is 510 Hz, what is a quite high frequency compared with experiments known from literature, so an important issue related to the seeding particles is their response time, which should be short enough to strictly follow acoustic movements. The characteristic response time of tracer particles can be computed by [14]:

$$T_p = \frac{(\gamma - 1) \cdot D^2}{18\nu}, \tag{12}$$

where: D is the seeding particle diameter, ν is the kinematic viscosity of the fluid and γ is the ratio of the density of a particle to the density of fluid. It is related to so-called particle terminal velocity [15]. If we take into consideration our experiment conditions (air at 25°C, ρ_{AIR}=1.18 kg m^{-3}, ν = 1.56 x 10^{-5} m^{2}s^{-1}, D=1 μm and $\gamma = \frac{\rho_{DEHS}}{\rho_{AIR}} = 770$), we obtain the value of T_p = 2.7 μs. For the pure tone of 510 Hz the particle response T_p is more than 700 times faster than the excitation signal period, so we could be sure that those seeding particles accurately follow the acoustic flow.

4. Experimental results and discussion

4.1 Correlation between the proposed model and experimental data - pure tone excitation

Particle image velocimetry is a complex measuring technique with many sources of errors. Detailed considerations about selected errors can be found in [1–4]. Their contribution to the total measurement accuracy is various and depends also on choice of the time interval Δt. For small Δt and resulting small displacements, the errors connected with insufficient spatial resolution of the system will dominate. If Δt increases, effects connected with velocity averaging over non-linear motion trajectory become noticeable. For long Δt, seeding particles can start to leave the interrogation areas, what also causes an increase of the displacement estimation error. It can be assumed that an optimum Δt value exists, and for that value the

presented systematic error should dominate. To examine this hypothesis an experiment was performed. The spatial distribution of the acoustic velocity vector was measured in a duct with pure tone excitation at 255Hz and 510Hz (wavelength λ of 1.35m and 0.653m). The instantaneous fields were recorded for 24 phases of the excitation tone period (50 image pairs for every phase). For 255Hz tone the experiment was repeated 24 times for a time interval value Δt from 163μs to 3912μs, in 163μs steps, that corresponds from 1/24 of T_{255Hz} to one T_{255Hz}. For 510 Hz tone the experiment was repeated 12 times in the same 163μs steps for time interval value Δt from 163μs to 1956μs that corresponds from 1/12 of T_{510Hz} to one T_{510Hz}.

The velocity field was measured on a 128mm x 128mm square. The spatial dimensions were less than 1/10 of λ_{255Hz} , therefore the RMS value of the recorded period of signal for each Δt was obtained using averaging velocity values over space and then their energy over all period phases.

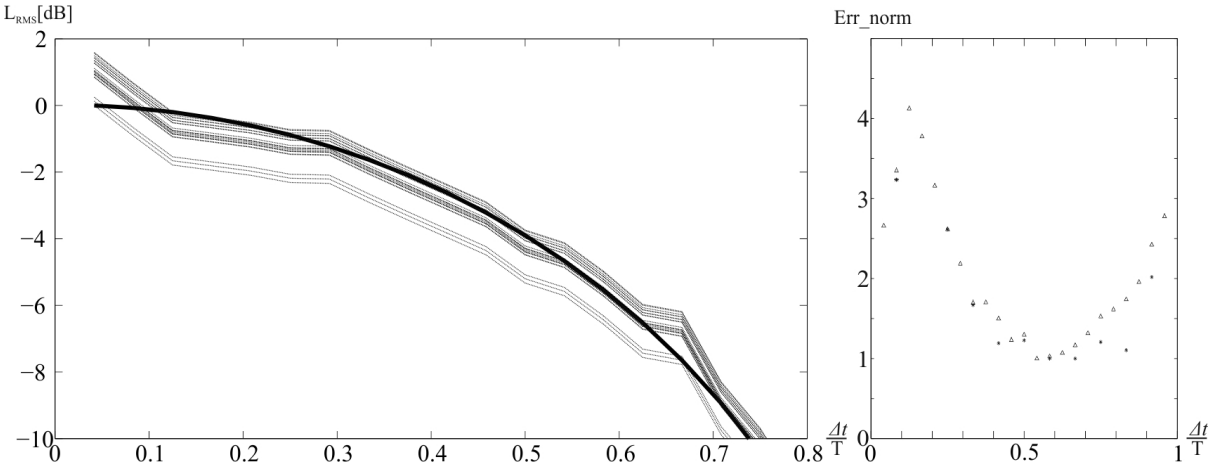

Fig. 5. The family of experimental results curves in reference to the model - bold line (left) and normalized fit error as a function of the measurement parameter $\Delta t/T$ (right).

Fig. 5 left shows the family of 255Hz tone measurement curves in a logarithmic scale, which are obtained by normalizing the real measurement curve by the consecutive values measured for different Δt. The normalized theoretical curve is shown as a bold line. In Fig. 5 right the root mean square fit errors (normalized to the minimum value) for both measurements are shown.

The best fit in both cases is obtained for Δt values of near half of the signal period. It can prove the thesis that in case when the PIV system registers the highest displacements, the inaccuracy in velocity evaluation due to optical resolution is minimal. The problem mentioned earlier of seeding particles which can go outside the interrogation areas, seems to be not dominant in case of acoustic movements whose amplitude is rather small comparing to the interrogation areas used in the algorithm for displacement computation.

The presented results affirm the measuring method presented in [12], but stay a bit in opposition to research presented in [5].

4.2 Application of a correction procedure to experimental data – dual-tone excitation

The spatial distribution of acoustic velocity was measured in the cross-section of a rectangular duct of 150mm x 150mm using the PIV system described above. As excitation signals pure tones of 255Hz and 510Hz and a dual tone (sum of two pure tones) with the same frequencies were used. For each excitation various Δt intervals were applied: Δt =980.4μs, what comprises $1/2T_{510Hz}$ and simultaneously $1/4T_{255Hz}$, Δt =1960.8μs, what is $1/2T_{255Hz}$ and

for Δt =490.2μs - 1/4T_{510Hz}, where T_{x_Hz} is the period of a harmonic signal of frequency x_Hz. Amplitudes of excitation tones were established in such a way that the measured sound pressure level in the area nearest to the investigated pressure anti-node for both frequencies was 130 dB SPL. The dual-tone signal was the sum of two pure tones with levels from the previous case. For every excitation signal the level of total harmonic distortions was monitored to keep the measurement in the linear range of loudspeaker performance. In such conditions the superposition principle remains valid. For every excitation case the signal period was divided into 24 steps (time resolution of 163.4μs, sampling rate about 6120 S/s) and for these phases instantaneous velocity values were evaluated as mean values from 25 image pairs recorded for each phase.

Fig. 6 shows the time series of measured instantaneous acoustic velocity in 4 points of the investigated plane (point coordinates: A(1,64), B(40,64), C(80,64) and D(110,64)).

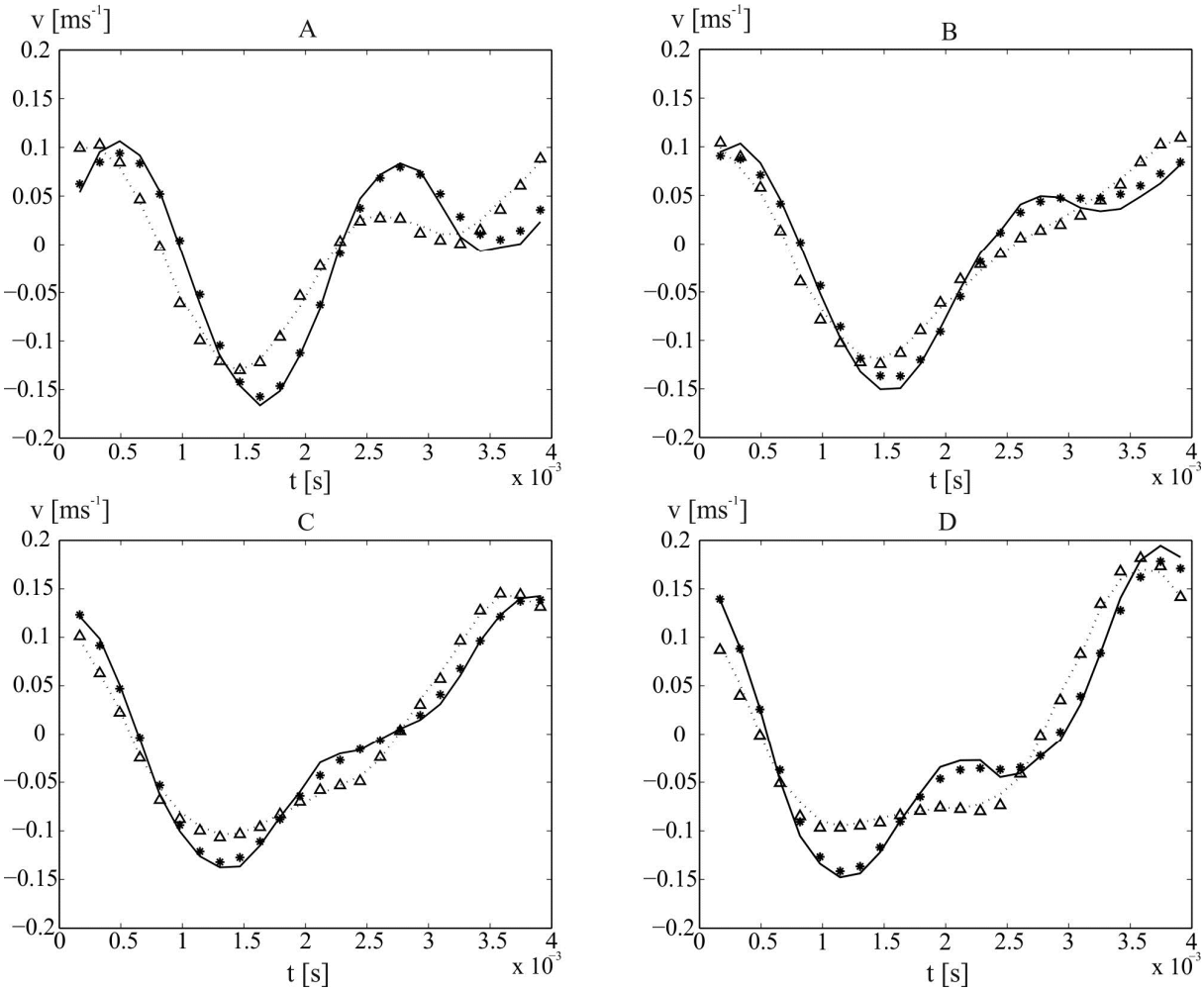

Fig. 6. Time series of measured acoustic velocity component *v* in 4 different space points (A, B, C, D). Dotted line (**..**) – dual-tone excitation; triangles (Δ) - the sum of measured values for pure tone excitation of 255Hz and 510Hz, Δt=980.4μs; solid line - the sum of measured values for pure tone excitation of 255Hz and 510Hz, constant $\Delta t/T$=4; asterisks (*) - result after correction procedure application to dual-tone measurement data.

In each point we observe different shapes of the acoustic velocity signal. It is caused by standing waves existing inside the tube and frequency-dependent space distribution of amplitudes and phases of harmonic components.

In the figures a dashed line (--) is used to show dual-tone excitation results, triangle points (Δ) for the sum of results obtained for pure tone excitation of 255Hz and 510Hz. For these three measurements the time interval was Δt =980.4μs. Taking into account the superposition rule, the results should be exactly the same. Some deviations could be caused by random errors and other non-linear phenomena occurring inside the duct. For the presented cases the relative RMS error was calculated as:

$$\varepsilon_{RMS} = \frac{v_{RMS\Sigma pure} - v_{RMSDuo}}{v_{RMSDuo}} \cdot 100\% , \tag{13}$$

where $v_{RMS\Sigma pure}$ is the RMS velocity value of the summed pure tone signals and $v_{RMS\ Duo}$ is the RMS velocity value of dual tone excitation.

The errors for presented cases were 1.2%, 2.7%, 1.9% and 3.6%. For all measured points the error was in the range of (-0.8;4.8)%, so it was less than 0.4dB. The solid line in Fig. 6 represents the sum of results obtained for pure tone excitation of 255Hz and 510Hz but with preserving the same ratio $\Delta t/T$=1/4. It is assumed that the accuracy level of velocity evaluation in this case is on the same level as in the previous case (values Δ), so it can be used as a reference for the robustness evaluation of the correction procedure being assessed.

The correction procedure for the dual-tone case is quite simple. When we use for a reference the sum of results obtained for pure tone excitation with constant ratio Δt/T=1/4, thus after doing FFT decomposition, we need only to correct the 510Hz component. It was measured with Δt/T=1/2, and should be corrected to $\Delta t/T$=1/4. Using (10) and (11) we need to calculate the amplitude and phase correction coefficients for both $\Delta t/T$, and correct the 510Hz component as follows:

$$v_{amp\_corr} = v_{amp} \frac{\varepsilon_{amp}(0.25)}{\varepsilon_{amp}(0.5)} \quad \text{and} \quad \varphi_{corr} = \varphi_0 - (\varepsilon_{phase}(0.5) - \varepsilon_{phase}(0.25)) . \tag{14}$$

The corrected results of dual-tone measurement are presented in Fig. 6 with an asterisk (*). Again the RMS errors were calculated between corrected results of dual-tone measurement and the sum of pure tone excitation with preserved $\Delta t/T$ ratio. Error values for these cases were 4.6%, 4.8%, 2.2% and 5.4%. For all measured points the error was in the range of (-0.16;8.8)%, so was less than 0.8dB. Without correction the error was in the range of (4;17)%, so it was even 1.4dB. As we can see, a correction procedure based on the presented systematic error model improves in an qualitative and quantitative manner the acoustic velocity field reconstruction based on phase-locked PIV measurement technique.

The results were also compared with measurements done using a well-established intrusive technique - hot wire anemometry. The measurements of acoustic velocity in the same model using sound intensity Microflown probe [16–18] stay with agreement with the corrected results presented above.

5. Conclusions

The working principle of particle image velocimetry causes that the acoustic particle velocity field measurement suffers from a systematic error introduced by non-zero time interval Δt. The measured sinusoidal signal is affected by multiplicative amplitude error and additive phase error. In the article a mathematical model of this error is presented, which can be used for the calculation of correction coefficients. Its application improves the obtained

results of visualization in a qualitative and quantitative way, what is shown experimentally. The proposed correction procedure allows more precise visualization of acoustic waves in time and space domains also for more complex excitation signals than pure tones. To the best knowledge of the author, the application of complex acoustical excitation signals in PIV experiments is not mentioned in literature. Further research will aim to use the PIV technique to observe acoustical phenomena caused by multitonal or band-limited noise excitation with a bandwidth of about 2 octaves, what seems to be possible looking at the presented research results. In conjunction with the non-intrusiveness of the PIV technique, it could be exploited for example in acoustic boundary layer research, development of new absorbing structures and many others.

Acknowledgements

The author like to express its gratitude to prof. Stefan Weyna for his scientific support and unconstrained access to his Image Laser Anemometry Laboratory at the Faculty of Maritime Technology and Transport of West Pomeranian University of Technology in Szczecin, Poland.

References

[1] Westerweel, J. (2000). Theoretical analysis of the measurement precision in particle image velocimetry. *Experiments in Fluids,* Suppl. S3–S12.

[2] Boillot, A., Prasad, A.K. (1996). Optimization procedure for pulse separation in cross-correlation PIV. *Exp. Fluids,* 21, 87–93.

[3] Raffel, M., Willert, C., Kompenhans, J. (2007). *Particle image velocimetry: a practical guide.* Springer, Berlin, New York, Heidelberg.

[4] Westerweel, J. (1993). *Digital particle image velocimetry - Theory and application.* Ph.D. Thesis. Delft University.

[5] Moreau, S., Bailliet, H., Valiere, J-Ch., Boucheron, R., Poignand, G. (2009). Development of Laser Techniques for Acoustic Boundary Layer Measurements. Part II: Comparison of LDV and PIV Measurements to Analytical Calculations. *Acta Acoustica united with Acoustica*, 95, 805–813.

[6] Hann, D. B., Greated, C. A. (1997). The measurement of flow velocity and acoustic particle velocity using particle image velocimetry. *Meas. Sci. Technol.* 1517–1522.

[7] Nabavi, M., Siddiqui, K., Dargahi, J. (2007). Simultaneous measurement of acoustic and streaming velocities using synchronized PIV technique. *Meas. Sci. Technol.*, 18, 1811–1817.

[8] Skulina, D.J., MacDonald, R., Campbell, D.M. (2005). PIV Applied to the Measurement of the Acoustic Particle Velocity at the Side Hole of a Duct. *Procedings of ForumAcusticum 2005.* Budapest.

[9] Tonddast-Navæi, A. (2005). *Acoustic Particle-Image Velocimetry Development and Applications.* Ph.D. Thesis. Open University, Milton Keynes, UK.

[10] MacDonald, R., Skulina, D.J., Campbell, D.M., Valiere, J.Ch., Marx, D., Bailliert, H. (2010). PIV and POD Applied to High Amplitude Acoustic Flow at a Tube Termination. *Procedings of 10-eme Congres Francais d'Acoustique,* Lyon.

[11] Nabavi, M., Siddiqui, K., Dargahi, J. (2008). Measurement of the acoustic velocity field of nonlinear standing waves using the synchronized PIV technique. *Experimental Thermal and Fluid Science*, 33, 123–131.

[12] Fischer, A., Sauvage, E., Röhle, I. (2008). Acoustic PIV: Measurements of the acoustic particle velocity using synchronized PIV-technique. *Proceedings* of *14th Int Symp on Applications of Laser Techniques to Fluid Mechanics.* Lisbon.

[13] Weyna, S., Mickiewicz, (2014). Phase-Locked Particle Image Velocimetry Visualization of the Sound Field at the Outlet of a Circular Tube. *Acta Physica Polonica A,* 125(4-A), A-108–112.

[14] Snyder, W.H., Lumley, J.L. (1971). Some measurements of particle velocity autocorrelation functions in a turbulent flow. *J. Fluid Mech.,* 48, 41–71.

[15] Siegel, D.A., Plueddemann, A.J. (1991). The motion of a solid sphere in an oscillating flow: an evaluation of remotely sensed Doppler velocity estimates in the sea. *J. Atmos. Ocean. Technol.*, 8, 296–304.

[16] Jacobsen, F., De Bree, H-E. (2005). A Comparison of two different sound intensity measurement principles. *J Acoust Soc Amer,* 118(3), 1510–1517.

[17] Weyna, S., Mickiewicz, W., Pyła, M., Jabłoński, M. (2013). Experimental acoustic flow analysis inside a section of an acoustic waveguide. *Archives of Acoustics*, 38(2), 211–216.

[18] Mickiewicz, W., Pyła, M., Jabłoński, M. (2011). Automatized system for 3D sound intensity field measurement. *Proceedings of 16th International Conference on Methods and Models in Automation and Robotics*. Międzyzdroje.